Organic-inorganic composites based on magnesium phosphate cement and acrylic latexes: Role of functional groups.

Lucie Zárybnická[a*], Jana Machotová[b], Petra Mácová[a], Alberto Viani[a]

[a]*Institute of Theoretical and Applied Mechanics of the Czech Academy of Sciences, Centre Telč, Prosecká 809/76, 190 00 Praha 9, Czech Republic*

[b]*Institute of Chemistry and Technology of Macromolecular Materials, Faculty of Chemical Technology, University of Pardubice, Studentská 573, 532 10 Pardubice, Czech Republic*

*** Corresponding author**: Alberto Viani (E-mail: viani@itam.cas.cz)

Institute of Theoretical and Applied Mechanics of the Czech Academy of Sciences, Centre Telč, Prosecká 809/76, 190 00 Praha 9, Czech Republic

Abstract

The role of carboxyl functional groups in acrylic latex employed to fabricate an organic-inorganic composite material based on magnesium phosphate cement has been investigated. At the beginning of the cement setting reaction, the acidic nature of the polymeric dispersion enhanced the dissolution of the magnesium oxide. During the following reaction steps, the rise in pH promoted the deprotonation of the carboxyl groups, which became involved in surface adsorption effects. They were found to control the nucleation and growth of the reaction products. This hindering effect slowed down the reaction rates and delayed the precipitation of the solid phosphates with beneficial consequences, namely, the retardation of setting time and the modulation of the heat released. Modification in the morphology of the formed crystals, with the prevalence of platelet-like over prismatic habit, along with a decrease in their average size, was obtained. Since the reaction proceeds closer to equilibrium, the crystals formed in a higher amount with respect to the neat cement. The resulting microstructure is strengthened because of a more effective intermingling between crystals and the amorphous phase. Furthermore, the synergistic combination of polymer and phosphate cement improved the elastic properties, and reduced the water absorption, impacting positively the durability of the composite.

Keywords: Magnesium Phosphate Cement; Acrylic Latex; Carboxyl Groups; Emulsion Polymerization

1 Introduction

Magnesium Phosphate Cements (MPCs), pertain to a group of chemically-bonded ceramics which harden at room temperature thanks to the reaction in water between magnesium oxide and an acidic phosphate (Abdelrazig et al., 1989). The interest in MPCs stems mostly from their

role as substitutes for Portland cement in some applications, in the context of the reduction of the environmental footprint of the cement industry (Abdelrazig et al., 1989; Hall et al., 2001), and also from their use as bone grafting materials, to overcome some of the downsides of Ca-P cements (e.g. poor mechanical performance, low resorption rate) (Wilson and Nicholson, 1993; Ostrowski et al., 2016).

In their most common formulation, magnesium oxide reacts with potassium dihydrogen phosphate (KH_2PO_4, KDP), leading to the formation of solid phosphate hydrate phases, as exemplified by the reaction (*Eq.* 1):

$$MgO + KH_2PO_4 + 5H_2O \rightarrow MgKPO_4 \cdot 6H_2O \qquad (Eq.\ 1)$$

The obtained ceramic body exhibits high compressive strength, but also a brittle mechanical fracture behavior, which is considered critical for some load-bearing applications (Ostrowski et al., 2016). In addition, owing to the high reaction rates and high temperature attained during the reaction, it is considered imperative to extend the setting time and modulate the release of heat (Wilson and Nicholson, 1993). None of the solutions proposed so far satisfy all these requirements. In fact, the research was mostly concentrated on the retardation of the setting reaction, for which boron-based compounds are largely employed as retarding additives (Sugama and Kukacka, 1983; Hall et al., 2001). In a recent work by the authors, it has been shown that the introduction of sub-micrometric acrylic polymers in the form of water-based dispersions (commonly known as latexes) may help in reducing the reaction rates, with a consequent extension of the working time (Zárybnická et al., 2021a). In addition, with respect to the neat MPC, the organic-inorganic composite material possessed better elastic properties, without detriment to the compressive strength. The synergistic combination of organic and inorganic components found its natural expression in this system, thanks to the compatibility of the MPCs reaction with the process of latex film-formation. In fact, the drying process, required to form the polymer film, occurs spontaneously during the setting reaction, because,

according to *Eq.* 1, water is progressively subtracted to be incorporated into the products. This marks a significant difference with other hydraulic binders, such as Portland cement, in which the introduction of latexes requires accurate control of curing conditions, since wet curing, which is beneficial to cement hydration, is of detriment for polymer film-formation (Frigione, 2013).

To date, there is still insufficient information about the nature of the interaction of the polymeric dispersion with the reacting MPC. Such information is essential to explain the influence of the organic component on the kinetics, the microstructure of the obtained composite and, in turn, its overall performance; all these aspects are of relevance for the effective design of MPC materials for applications.

In this respect, anecdotal evidence suggests that carboxyl (protonated) or carboxylate (ionized) groups attached to the latex particles' surface by copolymerization with methacrylic acid (MAA), may be active in the cement chemical environment, participating in ion complexation (in solution) and adsorption (at the surface of the newly formed reaction products) (Zárybnická et al., 2021a). Similar effects have been documented in Portland cement mortars (Ohama, 1987; Merlin et al., 2005) and Ca-P cements for biomedical applications (Mills, 2018), but no data are available for MPC.

To shed light on these aspects, taking advantage of the fact that the latex chemistry offers the possibility to modify the amount of surface functional groups, in this work, acrylic polymer latex compositions with different amounts of copolymerized monomer MAA, were synthesized to modulate the properties of MPC and obtain a mechanistic view of the processes involved in the interaction of the polymeric dispersion with the cement system. The impact on the rate of formation of the crystalline reaction product its weight fraction, crystal size and shape, and the consequences for the cement performance, have been described.

2 Experimental

2.1 Materials

The cement matrix was produced according to previous works (Zárybnická et al., 2021a; Zárybnická et al., 2021b) from KH_2PO_4 (KDP) (Penta, Czech Republic) and MgO obtained annealing $MgCO_3$ (Penta, Czech Republic) in an electrical furnace at 1600 °C for 40 min. Powders were obtained by milling in a Mini-Mill Pulverisette 23 (Fritsch, DE) and stored in a desiccator until use. Particle size parameters (CILAS LD 1090, CILAS, France) were: D_{10} = 0.72 µm, D_{50} = 3.97 µm and D_{90} = 10.73 µm, with Brunauer, Emmett and Teller (BET) specific surface (Asap 2020, Micromeritics, USA) area 2.805 $m^2 \cdot g^{-1}$ for MgO, and D_{10} = 5.18 µm, D_{50} = 26.19 µm and D_{90} = 81.45 µm for KDP.

Acrylic latexes were synthesized from methyl methacrylate (MMA), butyl acrylate (BA) and MAA. All the monomers were obtained from Sigma-Aldrich (Czech Republic). Disponil FES 993 (BASF, Czech Republic) was utilized as the surfactant, and ammonium persulfate (Penta, Czech Republic) was used as the initiator.

2.2 Synthesis of acrylic latexes

Three acrylic latexes, differing in the content of copolymerized MAA were prepared by a non-seeded emulsion polymerization of MMA and BA as the main acrylic ester monomers ordinarily used to produce commercial synthetic latex construction products. The proportions of monomers forming latex polymers (see Table 1) were chosen to achieve a calculated glass transition temperature (T_g), (using the Fox equation (Fox Jr and Flory, 1950)) of approximately 5 °C, in order to ensure film-formation at the common temperatures of MPC reaction.

Different amounts of carboxyl groups were incorporated into latex samples (2, 4, and 6 wt. % of MAA in the monomer mixture, which are commonly used concentrations in acrylic ester copolymer dispersions). Due to the highly hydrophilic nature, the carboxyl groups are believed to be located predominantly on the surface of polymer particles (Yeliseyeva et al., 1973).

A schematic representation of the structure of acrylic polymers is illustrated in Fig. 1.

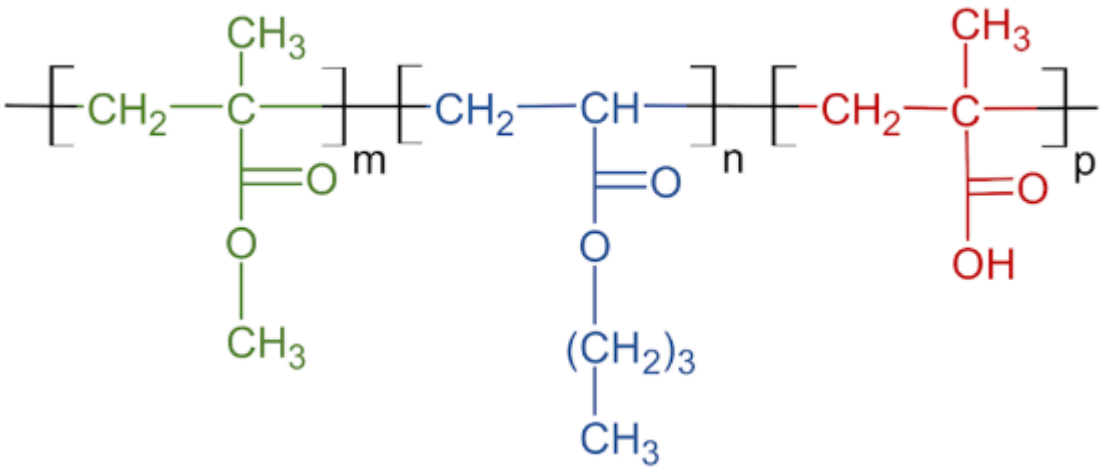

Fig. 1. Schematic illustration of acrylic latex polymers; ***m***, ***n*** and ***p*** identify the proportions of MMA, BA and MAA monomer units, respectively.

The latexes were produced in a 500 mL glass reaction flask under a nitrogen atmosphere at a polymerization temperature of 85 °C. The reaction flask charge (consisting of distilled water, initiator, and surfactant) was put into the reaction flask and heated to the polymerization temperature. The monomer emulsion was consequently dosed into the stirred reaction flask at a dosing rate of about 2 $mL.min^{-1}$. The polymerization was then completed, during the 2 hours of the hold period.

Table 1. Composition of acrylic latexes.

Sample	Composition of monomer feeds / g MMA/BA/MAA
2MAA	84/112/4
4MAA	80/112/8
6MAA	76/112/12

A detailed recipe of the emulsion polymerization system is presented as Supplementary Material Table S1. According to the chemistry of the early stages of the MPC setting reaction (Soudée and Péra, 2000), the pH of all latexes was adjusted to 4 by employing an ammonia solution. The prepared acrylic latexes were named according to the different amounts of MAA used, namely 2MAA, 4MAA and 6MAA.

2.3 Preparation of cement composites

The reference MPC samples were produced by mixing 6.078 g KDP, 3.150 g MgO, and 4.023 g of deionized water to attain a water-to-solid weight ratio of 0.44. The slurry was then poured in silicone moulds (1×1×1 cm to obtain specimens for compressive strength tests). Similar to previous works (Zárybnická et al., 2021a; Zárybnická et al., 2021b), such cement formulation contains a stoichiometric amount of water and KDP, with respect to *Eq.* 1, whereas MgO is in excess of KDP (MgO/KDP molar ratio 1.75). The composites were produced with the same amounts of reagents by adding 5 wt.% of latex polymer, calculated according to the polymer solid content of each latex dispersion. This amount was found adequate to improve MPC properties, according to already published results (Zárybnická et al., 2021a), and is in line with other formulations adopted for latex-modified Portland cement mortars since it allows an adequate film formation within the matrix (Beeldens et al., 2005; Tukimat et al., 2017; Jin and Stephan, 2019). All samples were demolded after one day and aged at room temperature for 27 days before tests. Samples are marked as MPC (reference) and MPC_**x**MAA, where **x** is the amount of MAA.

2.4 Methods

2.4.1 Characterization of latexes and their polymers

The solid content of latexes was measured according to ISO 3251 (Anon, 2003). The average particle size and zeta potential of latex samples were measured by dynamic light scattering (DLS) on a Coulter N4 Plus instrument (Coulter, Corp., UK). The DLS measurements were

done at 25 °C. The concentration of measured latex samples was approximately 0.05 wt. % of solids.

The minimum film-forming temperatures (MFFT) of the latexes were determined according to ISO 2115 (Anon, 1996), using the MFFT-60 instrument (Rhopoint Instruments, UK). The MFFT is defined as the minimum temperature at which a film cast from a polymer dispersion becomes continuous and clear.

2.4.2 Characterization of cement composite reaction

Isothermal conduction calorimetry (ICC) was adopted to follow the heat signal during the cement reaction. The powder (MgO and KDP) and the liquid (water or water with latex dispersion) were kept separated in an Ad-Mix® ampoule. The experiment started with the injection of the liquid onto the powder after they had been equilibrated at the nominal temperature of the experiment (25 °C). The slurry was mixed for 120 s and the heat flow was recorded with a TAM-Air (TA Instruments, DE) 8-channel instrument for 48 h.

2.4.2 Characterization of MPC samples

Quantitative phase analysis of the dried ground samples was conducted through Rietveld refinements of X-ray powder diffraction (XRPD) data, collected in the angular range 14–70° 2θ, counting 0.4 s for each step of 0.0102° 2θ on a Bruker D8 Advance (Bruker AXS) Bragg–Brentano θ-θ diffractometer equipped with a LynxEye 1-D silicon strip detector, adopting Cu Kα radiation (λ=1.5418 Å). Before the measurement, the polymer fraction was extracted from the cement matrix by soaking for 24 h in tetrahydrofuran under sonication. The quantification of the amorphous phase was obtained by spiking the samples with 10 wt.% of ZnO as the internal standard, calibrated on corundum standard material (NIST SRM 676a). Rietveld refinements for Quantitative Phase Analysis (QPA) were performed by adopting the fundamental parameter approach with the software TOPAS 4.2 (Bruker AXS) (Viani and Gualtieri, 2014; Viani et al., 2015).

The ceramic composite microstructure was investigated after 28 days of ageing by means of a scanning electron microscope (SEM). Exposed internal surfaces, gold coated with a 7 nm thick layer were observed in backscatter mode at 90 Pa pressure and accelerating voltage 20 kV, adopting a Quanta 450 FEG (FEI, Czech Republic) instrument.

In absence of specific standards for compressive strength tests on this class of materials, the procedure adopted in previous works (Zárybnická et al., 2021a; Zárybnická et al., 2021b; Cárdenas et al., 2021) was followed. Tests were conducted after 28 days on the cubic specimens at a speed of 0.2 $mm \cdot min^{-1}$ and a maximum load of 5 kN with an Instron 3345 (Instron, USA) instrument. Five replicates were tested for each sample.

2.4.3. Latex adsorption kinetics test

The affinity of latex dispersions for the crystalline component of the cement (i.e. MKP) has been investigated by an adsorption kinetics test. MKP was synthesized as described elsewhere (Zhang et al., 2013) by mixing $MgCl_2$·KDP and KOH, purchased from Penta (Czech Republic), in boiled deionized water,. The quality of the product of synthesis was assessed by the XRPD method.

The adsorption kinetics tests were conducted in batches. Each sample was prepared by dispersing 50 mg of MKP in 25 mL of a water solution containing 200 $mg \cdot L^{-1}$ of latex in sealed polyethylene bottles. The pH was brought to 9 with an 8M KOH. The suspensions were equilibrated by agitation in a digital orbital shaker (Heathrow Scientific, USA) at 25 °C. Samples were collected at different times (0, 10, 30, 50, 110, and 230 min) to measure the amount of latex adsorbed at the solid surface, which was expressed as a depletion of the polymer from the solution (Rosen and Kunjappu, 2012). The supernatant was separated by centrifugation; to avoid latex separation, optimal conditions were found to be 5 min at 4000 rpm. Latex concentration was measured using a visible (VIS) spectrophotometer DR3900 (HACH, USA). For the purpose of this study, it was considered adequate to fit the plot of the

amount of adsorbate vs. time to the pseudo-first-order model, to retrieve the rate of adsorption and the equilibrium concentrations (William Kajjumba et al., 2019).

3 Results and discussion

3.1 Latexes

Properties of the synthesized acrylic latexes are listed in Table 2. The latexes, having a solid content of around 39 wt. %, comprised polymer particles of a diameter of about 120–140 nm, which represents a typical latex particle size (Hanus et al., 2001). The values of zeta potential indicate stable latex formulations and are in line with similar materials synthesized with the use of anionic surfactants and a persulfate initiator (Behrens et al., 2000). Notably, the increasing content of copolymerized MAA resulted in the enhancement of the negative zeta potential, which indicates an increased surface charge due to the presence of a higher number of carboxyl acid groups on the polymer particle surface.

It is also worth mentioning that all the prepared latex samples exhibited low MFFT values, which suggests high mobility and penetration ability of the latex polymers, aspects which favor adhesion and cohesion of the resulting cement composites, in a wide range of cement application temperatures.

Table 2. Characteristic properties of the acrylic latexes.

Sample	Solids / wt.%	Particle size / nm	Zeta potential / mV	MFFT / °C
2MAA	39.5 ± 0.1	130.5 ± 2.4	-30.2 ± 1.6	< 0
4MAA	40.1 ± 0.1	137.9 ± 3.8	-34.5 ± 0.5	< 0
6MAA	39.7 ± 0.2	123.4 ± 2.4	-39.0 ± 0.5	< 0

3.2 Monitoring of setting reaction

Fig. 2 illustrates the heat flow curves normalized to the amount of MgO for the investigated samples, limited to the first hour, for sake of clarity. Without polymer, a broad signal of heat

evolution is observed. According to the literature, at least two main events of heat release can be identified (Viani and Mácová, 2018): the first one corresponds to the dissolution of MgO and is caused by the acidic pH attained when KDP dissolves in solution; KDP dissolution in water gives an endothermic contribution which is largely masked by the much higher heat evolved during oxide dissolution. Another exothermic event is usually assigned to the crystallization of the phosphate hydrate (MKP). Between these two episodes of heat evolution, an additional component is present, which was found to correspond to the formation of an amorphous precursor of MKP (Sotiriadis et al., 2018; Viani and Mácová, 2018).

The presence of the polymeric emulsion is slightly delaying the onset of MgO dissolution, preceded by a slowdown of the dissolution of KDP. In both cases, the effect is enhanced by the amount of carboxyl groups in the latex. This phenomenon can be ascribed to different levels of ionic strength in the reaction environment. The latex-modified cement samples contained ammonia, which was added in a certain amount to the latex to adjust the pH to 4; the more copolymerized MAA, the more ammonia was consumed and the higher ionic strength was introduced, decreasing ionic mobility and extending the time to MgO dissolution (Amaral et al., 2010), as can be seen from the graph in Fig. 2. However, the oxide dissolution proceeds at slightly higher rates, compared to the neat MPC. In fact, the first maximum in the heat flow curves is always higher with respect to the reference sample. The calculation of the total heat released during this step is hampered by signal broadening and by the presence of the overlapping contribution of the amorphous intermediate, whose signal is ‘hidden’ between the two main peaks (Viani and Mácová, 2018). As previously observed (Zárybnická et al., 2021a), the increase in the rates of MgO dissolution is likely the result of the slightly lower pH of the polymeric dispersion (pH = 4.0) with respect to the solution of neat KDP (~4.3).

During these first minutes, because of the acidic chemical environment, the role of carboxyl groups on the latex particles should not be relevant, due to their low degree of deprotonation

(Zárybnická et al., 2021b). However, with the release of Mg^{2+} ions into the solution, the pH increases quickly (Bayuseno et al., 2020) and the carboxyl groups should actively interfere with the next reaction steps. In fact, when the second exothermic peak (conventionally assigned to the crystallization of MKP) is considered, a remarkable retarding effect of the polymer, which can be quantified in about 15-20 min, is observed. The effect is correlated with the density of carboxylate functional groups since the maximum slightly shifts at later times increasing the MAA content. The rates of heat evolution also increase with increasing the amount of MAA in the latex, but the heat is released more gradually during this event, as indicated by the broadening of the heat flow peak.

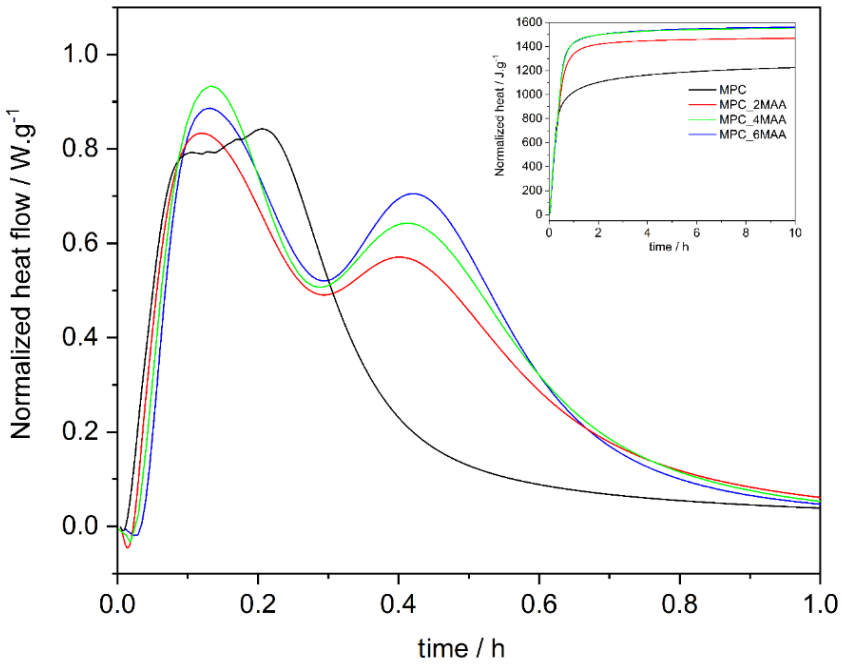

Fig. 2. The plot of the normalized heat flow in the first 60 min for the investigated samples. Inset illustrates the normalized heat during the first 10 hrs.

In complex, the total heat released at the end of the experiment, normalized to the amount of MgO, increases increasing the amount of the carboxyl groups (see Table 3 and inset in Fig. 2), whereas the reference sample exhibits the lowest value. The retarding effect on the crystallization of MKP, which is beneficial because of the extension of the working time (which

correlates with the time of the corresponding maximum in the heat flow trace (Abdelrazig et al., 1989; Hall et al., 2001; Zárybnická et al., 2021a)), is in agreement with recent tests on latex-modified MPC (Zárybnická et al., 2021a).

Table 3. Normalized heat released at the end of the experiment normalized to MgO content.

Sample	Normalized heat / $J \cdot g^{-1}$
MPC	1 265
MPC_2MAA	1 481
MPC_4MAA	1 577
MPC_6MAA	1 581

The signal overlap in the ICC trace, previously mentioned, prevented the exact quantification of the effect of the amount of MMA on the crystallization step, therefore, more insights into this aspect will be gained by analyzing the phase composition of the ceramic composite, as described in the next section.

3.3 Ceramic composite phase assemblage

The results of quantitative phase analysis with the Rietveld method of samples aged 28 days are summarized in Table 4, whereas powder diffraction patterns and an example of graphical output of Rietveld refinement are provided as Supplementary Material Fig. S1. All samples are composed of three phases: MKP, residual MgO, and a fraction of the XRPD amorphous phase. This is in agreement with other previous results (Viani et al., 2015; Viani et al., 2016a; Viani et al., 2016b; Viani et al., 2017; Zárybnická et al., 2021a).

The polymer promoted both MgO dissolution and MKP crystallization, consistently with the higher amount of heat released in presence of latex during the ICC experiment. It is worth noting that MgO dissolution was more pronounced at high content of MAA, therefore, it was positively correlated with the amount of carboxyl groups.

When the MKP content is considered, on one side, the composites exhibit a higher amount of MKP with respect to the neat MPC; on the other side, the increase in the amount of carboxyl groups exerted a progressive inhibiting effect on crystallization. The absolute changes in MKP content are higher with respect to the variations observed in the amount of MgO, consequently, the amorphous content exhibits opposite trends, being more abundant in the samples containing latexes with the highest amount of carboxyl groups.

Table 4. Results of QPA for the samples after 28 days.

Sample	MgO / wt.%	MKP / wt.%	Amorphous / wt.%
MPC	9.4 ± 0.1	46.2 ± 0.1	44.4 ± 0.7
MPC_2MAA	8.0 ± 0.1	53.0 ± 0.1	39.0 ± 0.7
MPC_4MAA	8.0 ± 0.1	52.8 ± 0.1	39.1 ± 0.6
MPC_6MAA	5.9 ± 0.1	49.3 ± 0.1	44.9 ± 0.6

The results of QPA can be compared only from a qualitative standpoint to those obtained during the isothermal calorimetric tests, because of the already mentioned strong overlap of the heating events in the ICC trace and the impossibility of disentangling the contribution to the heat flow curves of each one of the three main heating events, due to the lack of accurate analytical expressions to describe the signal. Concerning the dissolution of MgO, higher rates and broader signals confirmed the enhanced dissolution detected with XRD in the composites with respect to the neat cement. The higher solubility of MgO correlates with the increasing MAA content, also confirmed by ICC analysis. As for the MKP, it is well documented that lower crystallization rates lead to a higher amount of MKP because the reaction proceeds closer to equilibrium (Viani and Mácová, 2018; Viani et al., 2020). Under such conditions, the total heat released at the end of the reaction is expected to increase (see Fig. 3 and Table 3). The concomitant decline in MKP content increasing the amount of carboxyl groups located on the surface of latex particles should find an explanation in the interaction of the polymer with the cement reaction, which will be discussed later.

3.4 Cement microstructure, mechanical and physical properties

The microstructure of the composites, visible under SEM (Fig. 3), is dominated by the large crystals of MKP in the ceramic matrix (frequently > 20 µm). This is a peculiar feature of the MPC microstructure, as well illustrated in the reference sample (Fig. 3a). The MKP crystals were usually densely packed and embedded in the amorphous phase. In backscatter mode both phases displayed the similar distribution of grey levels, indicating a similar chemical composition. This should be expected, as the amorphous phase has been identified as a Mg-phosphate hydrate with structural affinity with MKP and hosting the same structural units (Viani et al., 2017).

In the latex-modified samples, the polymer exhibited a relatively even distribution, adhering to the MKP individuals, gluing them together or bridging between crystals (Fig. 3b, d). Similar behavior is observed in polymer-modified Portland cement mortars (Knapen and Van Gemert, 2015). No evidence of reaction rims or corrosion effects, suggesting dissolution or chemical reaction with MKP, was detectable.

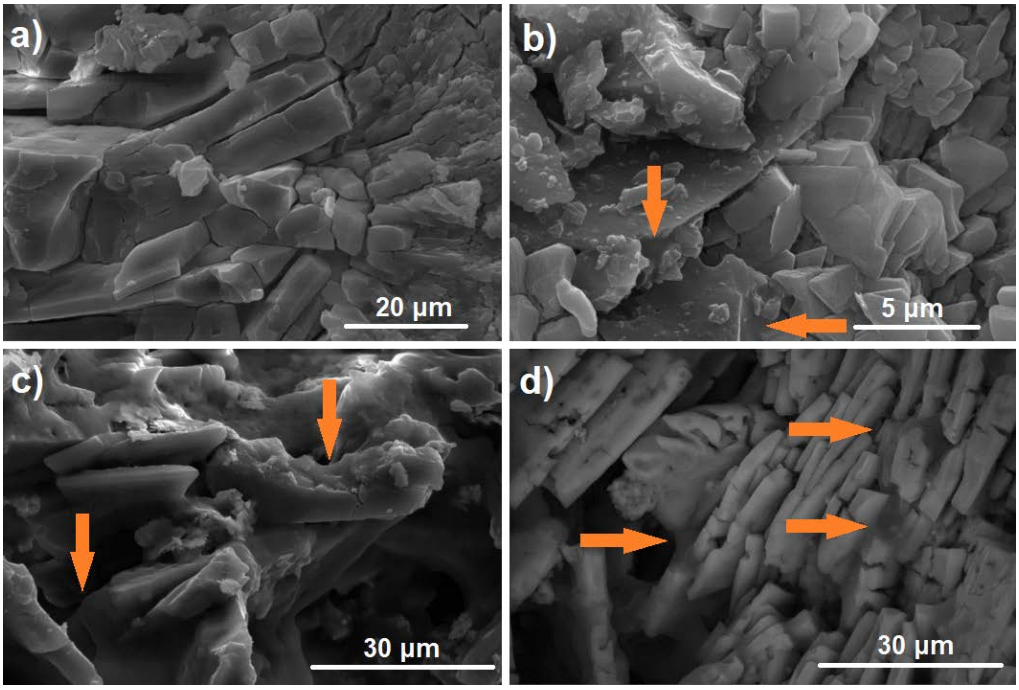

Fig. 3. Gallery of SEM micrographs illustrating the microstructure of the prepared samples: a) MPC; b) MPC_2MAA; c) MPC_2MAA; d) MPC_6MAA. Arrows indicate the local concentration of polymer.

In MPC, MKP is known to take both prismatic elongated and platelet-like crystal habits (Viani et al., 2016b; Viani et al., 2020; Zárybnická et al., 2021a). Crystallization and microstructural studies showed that at lower reaction rates, the platelet-like morphology prevails (Abdelrazig et al., 1989; Viani et al., 2016a; Viani and Mácová, 2018; Zárybnická et al., 2021a). This crystal habit was the most frequently detected in the polymer-modified samples, also illustrated in Fig. 3d. This is in agreement with the lower overall crystallization rates, with respect to the neat MPC, recorded with ICC.

In the latex-modified MPC, other two remarkable microstructural modifications were recorded. One is the local concentration of the polymer inside voids (see Fig. 3b, d). The pore-filling ability of polymer additives is documented in latex-modified Portland cement mortars as well as MPCs, and has been considered a strengthening mechanism in these composites, especially when the flexural strength is concerned (Zhang et al., 2004; R. Wang et al., 2005; P. M. Wang et al., 2005; Tukimat et al., 2017; Zárybnická et al., 2021a; Zárybnická et al., 2021b).

The second remarkable microstructural feature is the decrease in the average size of MKP crystals. The latter effect was previously reported in MPC modified with PVA and styrene-butadiene latex (Zárybnická et al., 2021a; Zárybnická et al., 2021b) and it is strictly connected with the chemical-physical interaction of the polymer with the MPC reaction that will be discussed in detail in the next section.

Notably, sub-spherical pores, indicative of air entrapment, are absent. They have been frequently reported in latex-Portland cement composites, where they are detrimental to mechanical performance (Tian et al., 2013).

Table 5 summarizes the results of mechanical and physical properties of the studied samples. The latex-MPC composites exhibited lower water absorption, compared to the reference, confirming the beneficial effect of the pore-filling ability of the polymer, which reduced the apparent porosity. However, the improvement was progressively reduced with the increase in the amount of carboxyl groups This can be due to the hydrophilic behavior of the polymer, which increases with the amount of MAA, and leads to an increase in the amount of water entrained into the composite matrix (Wang and Pan, 2002).

When the compressive strength is considered, the composites performed better than the neat MPC. In this case, the strength increased with the amount of carboxyl groups in the latex. This trend should arguably be attributed to the modifications induced on the composite microstructure by the carboxyl groups, namely, the reduction in the amount and size of MKP crystals and the alteration of the crystal morphology. The main toughening mechanism in MPC has been recognized to be the growth of an interlocked microstructure of MKP crystal embedded in the amorphous matrix (Ding et al., 2012; Viani et al., 2016b; Viani et al., 2020). Although crystals are usually performing better that the amorphous counterpart, which explains why, overall, the composites overperform the neat MPC (containing a lower fraction of MKP), it can be conjectured that the improved performance increasing the amount of carboxyl groups in the polymer, resulted from the concomitant change in prevalent crystal habit and the reduction in amount and size of crystals, which led to the formation of more effective microstructures. Further studies are needed to prove/disprove this hypothesis.

Table 5. Results of water absorption, and compressive strength test for the investigated samples after 28 days.

Sample	Water absorption / wt. %	Compressive strength / MPa
MPC	6.20±0.2	26.2±7

MPC_2MAA	2.28±0.3	26.2±8
MPC_4MAA	3.65±0.2	33.2±14
MPC_6MAA	5.52±0.4	40.8±12

The load-displacement curves recorded during the compressive strength tests (see Fig. 4) showed that the neat MPC is characterized by a marked brittle behavior with limited elastic and plastic deformation. Conversely, all the polymer-cement composites exhibit significant ductility, which is the ability to undergo large plastic deformation before final failure. This is likely related to the latex-cement adhesion and intrinsic elastic properties of the latex. The contribution of the polymer additive to the elastic behavior of the composite was further confirmed by the progressive extension of the elastic region in the load-displacement curves when the MAA content is increased from 2 to 6 wt.%. In fact, methacrylic acid has been already observed to impart better elastic properties to the polymer film (Mohammed et al., 1997). The enhanced elastic behaviour is a peculiar aspect of the cement-polymer composites, as previously documented in Portland cement or MPC in presence of styrene-butadiene and acrylic latexes (Lavelle, 1988; Rossignolo and Agnesini, 2002; Zárybnická et al., 2021a).

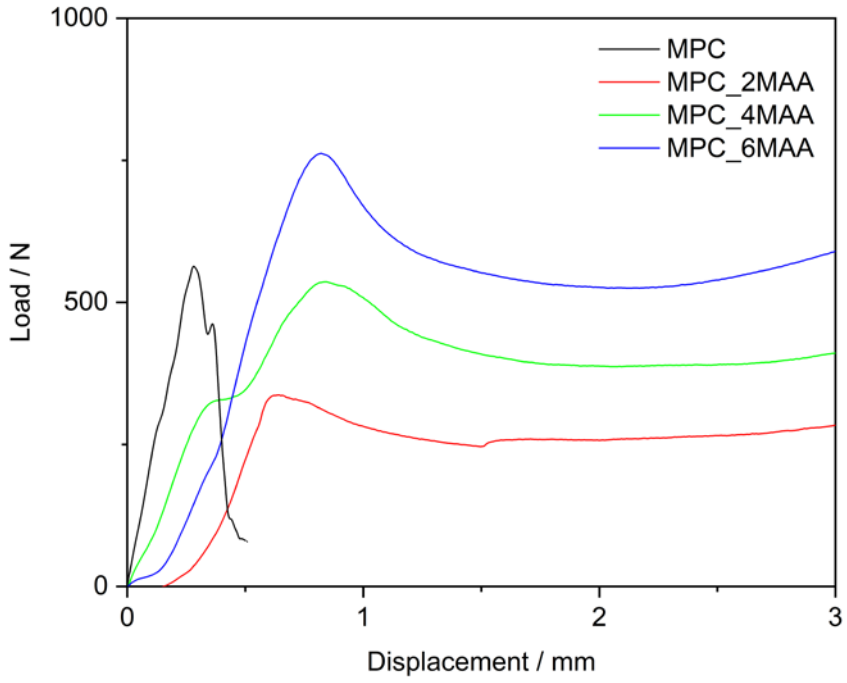

Fig. 4. Load-displacement curves for a set of samples of MPC and latex-modified MPC.

3.5 Cement-additive interaction and final considerations

The results presented so far indicated that the cement-latex interaction is controlled by a combination of chemical and physical effects. During the first reaction stages, MgO dissolution is enhanced because latex dispersion contributes to decrease the pH. At low pH the oxide surface is unstable and dissolution is promoted by the nucleophilic attack of protons (Fruhwirth et al., 1985). With the progressive release of Mg^{2+} ions in solution, the pH rises, and so does the deprotonation level of the carboxylate functional groups located on the surface of the latex particles (Zhang et al., 2003).

Therefore, the metal ions may become the target of adsorption by the latex particles, but they can be also subtracted by the nucleating phosphates. In the first case, the apparent supersaturation level of Mg^{2+} ions is reduced; in the second case, the nuclei of the newly formed phosphates provide adsorption sites for the latex particles. Both ways, the net effect is the hindered nucleation and growth of phosphates, as evidenced by ICC and confirmed by XRPD. Similar mechanisms were previously described for latex-modified Portland cement and MPC modified with polyvinyl alcohol (PVA) (Plank and Gretz, 2008; Lu et al., 2018; Zárybnická et al., 2021b), but thermodynamic arguments indicated that adsorption effects at solid surfaces largely prevails over complexation in solution in control the retardation. The affinity of the latex for the MKP crystal surface has been confirmed by the adsorption kinetic tests conducted on the synthesized MKP. Fig. 5 illustrates an example of a plot of adsorption capacity as a function of time, which allowed to obtain the values of adsorption capacity at equilibrium (Q_e) and the rate of adsorption, reported in Table 6. Similar results have been obtained for carboxylate-containing moieties adsorbed on struvite, the ammonia isostructural form of MKP (Kofina et al., 2007; Prywer et al., 2015; Wei et al., 2019; Polat and Sayan, 2020).

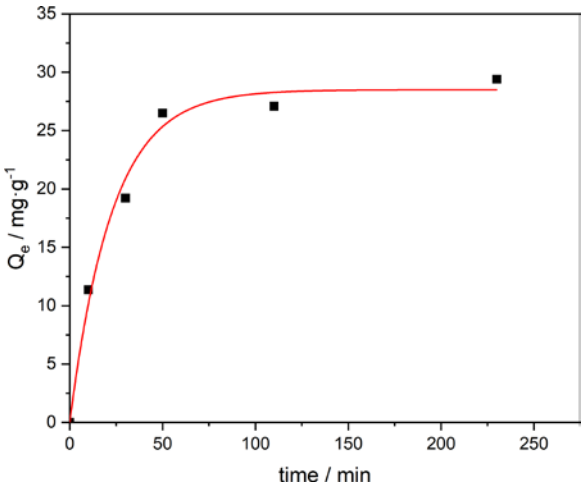

Fig. 5. Evolution of acrylic latex (2MAA) adsorption on MKP crystals with time.

In general, when the surface of the adsorbent is constant, the adsorption of larger molecules is less affected by changes in the number of active sites (Schulthess and Tokunaga, 1996). It is therefore not surprising that Q_e doesn't exhibit significant trends in function of the MAA content. When the apparent rates of adsorption are considered, they are very similar within the error of the measurement, irrespective of the density of carboxyl groups.

Table 6. Parameters obtained from the adsorption kinetics experiments.

Sample	Q_e / mg·g^{-1}	Rate / (mg·g^{-1})·min^{-1}	R^2
2MAA	28.5 ± 1.0	0.044 ± 0.003	0.988
4MAA	29.6 ± 1.2	0.030 ± 0.006	0.984
6MAA	30.3 ± 0.9	0.037 ± 0.009	0.989

It should be pointed out that the interaction of the latex with the MPC system cannot be entirely explained by the results of the adsorption kinetic experiments, since the mutating conditions occurring during the setting reaction could not be exactly reproduced. Crucial in this respect is the presence of the metastable amorphous phase and the role of the reaction kinetics. The polymer hindered the growth of nuclei of critical size, consistently with the lower rates and

the delayed crystallization peaks recorded with ICC. But, as discussed above, lower overall rates shift the reaction towards thermodynamic instead of kinetic control, favoring the amorphous-to-crystalline transformation, therefore enhancing the amount of MKP. This is due to the fact that at lower rates the ion mobility is preserved for longer times, a condition which is essential to the structural rearrangements needed to establish the long range order to form the MKP (Viani and Mácová, 2018; Viani et al., 2020).

In other words, on one hand, in all the samples the phase fraction of MKP is higher than in the reference because of the beneficial effects of the lower rates (Viani and Mácová, 2018; Viani et al., 2020).On the other hand, surface adsorption helps in stabilizing the amorphous intermediate phase, similarly to what has been reported for the amorphous-to-crystalline transformation in PVA-modified MPC (Zárybnická et al., 2021b) and in Ca-phosphates precipitated in presence of carboxyl groups (Chatzipanagis et al., 2016). This explains the progressive increase in the amorphous fraction, increasing the amount of carboxyl groups. Hindered crystallization effects have been already observed during the crystallization of struvite from solution in presence of molecules containing carboxyl groups (Kofina et al., 2007; Prywer et al., 2015; Polat and Sayan, 2020).

The precipitation experiments of struvite also evidenced a tendency towards the decrease in average crystal size with the increase in concentration of active molecules, and modifications in the morphology of the obtained crystals. An analogy can be drawn between the former effect and the results of SEM observations in the MPC samples, pointing to a reduced size in the composites. The overrepresented platelet-like morphology in these samples should be attributed to the lower overall rates attained (this crystal habit is not obtained in solution).

Therefore, the affinity of the carboxyl groups for the newly formed surfaces and the growing solid products modified the reaction path acting on the interplay between kinetic and

thermodynamic factors, ultimately affecting the development of the cement microstructure, and, consequently, the measured compressive strength.

It can be concluded that the beneficial effects in terms of mechanical performance, elastic properties, water absorption, modulation of heat evolution and mitigation of the reaction ratesare obtained thanks to the physical-chemical interaction of the carboxyl moieties with the MPC system and the synergistic effect obtained by coupling the cement and the polymer.

4 Conclusions

The modification of magnesium phosphate cement with acrylic latex polymer hosting different amounts of carboxyl functional groups has been studied. Thanks to the flexibility of latex chemistry, macromolecules hosting different amounts of surface carboxyl groups were synthesized. The following conclusions can be drawn:

The polymeric dispersion enhanced the first dissolution of metal oxide, arguably because of its low pH.

The successive reaction steps were more affected by the presence of the polymer because of the increased deprotonation of the carboxyl groups, which became involved in adsorption processes. Surface adsorption was considered to hinder nucleation and growth of reaction products, in analogy with other systems, such as Portland cement and Ca-P cements.

The net effect was to delay and slow down the precipitation of the magnesium phosphate hydrates and the conversion of the amorphous intermediate phase into the crystalline phosphate.

Nonetheless, the mitigation of the rates (which has beneficial effects on the cement working time) shifting the reaction towards equilibrium, promoted the formation of a higher amount of crystalline product with respect to the neat cement and caused the platelet-like morphology of crystals to prevail over the acicular-needle-like one.

The affinity of latex particles for the crystal surfaces was considered the reason for the reduced size of the crystals in the composites and the progressive reduction of the crystalline fraction increasing the density of carboxyl groups in the polymer. The former effect is likely leading to a stronger microstructure, where crystals and amorphous phase are more effectively intermingled since the compressive strength is higher with respect to the neat cement.

The cement matrix and the polymer additive operate in a synergistic fashion thanks to the complementarity of their mechanical properties, which imparted ductile behaviour to the composite, and the pore-filling ability of the additive, which reduced the water absorption of the composite.

Acknowledgements

This study was supported by the Czech Science Foundation GA ČR (Grant Number 20-01280S) and by the Czech Academy of Sciences, Institute of Theoretical and Applied Mechanics (RVO 68378297).

References

Abdelrazig B. E. I., Sharp J. H. and El-Jazairi B. (1989) The microstructure and mechanical properties of mortars made from magnesia-phosphate cement. *Cem. Concr. Res.* **19**, 247–258.

Amaral L. F., Oliveira I. R., Salomão R., Frollini E. and Pandolfelli V. C. (2010) Temperature and common-ion effect on magnesium oxide (MgO) hydration. *Ceram. Int.* **36**, 1047–1054.

Anon (2003) *ČSN EN ISO 3251 (673031) Nátěrové hmoty - Stanovení netěkavých podílů nátěrových hmotách a pojivech pro nátěrové hmoty.*,

Anon (1996) *ISO 2115:1996 Plastics — Polymer dispersions — Determination of white point*

temperature and minimum film-forming temperature.,

Bayuseno A. P., Perwitasari D. S., Muryanto S., Tauviqirrahman M. and Jamari J. (2020) Kinetics and morphological characteristics of struvite (MgNH4PO4.6H2O) under the influence of maleic acid. *Heliyon* **6**, e03533.

Beeldens A., Van Gemert D., Schorn H., Ohama Y. and Czarnecki L. (2005) From microstructure to macrostructure: An integrated model of structure formation in polymer-modified concrete. *Mater. Struct. Constr.* **38**, 601–607.

Behrens S. H., Christl D. I., Emmerzael R., Schurtenberger P. and Borkovec M. (2000) Charging and aggregation properties of carboxyl latex particles: Experiments versus DLVO theory. *Langmuir* **16**, 2566–2575.

Cárdenas C., Mácová P., Gómez M., Zárybnická L., Ševčík R. and Viani A. (2021) Formation, Properties, and Microstructure of a New Steel Slag–Based Phosphate Cement. *J. Mater. Civ. Eng.* **33**, 04021330.

Chatzipanagis K., Iafisco M., Roncal-Herrero T., Bilton M., Tampieri A., Kröger R. and Delgado-López J. M. (2016) Crystallization of citrate-stabilized amorphous calcium phosphate to nanocrystalline apatite: a surface-mediated transformation. *CrystEngComm* **18**, 3170–3173.

Ding Z., Dong B., Xing F., Han N. and Li Z. (2012) Cementing mechanism of potassium phosphate based magnesium phosphate cement. *Ceram. Int.* **38**, 6281–6288.

Fox Jr T. G. and Flory P. J. (1950) Second-order transition temperatures and related properties of polystyrene. I. Influence of molecular weight. *J. Appl. Phys.* **21**, 581–591.

Frigione M. (2013) Concrete with polymers. In *Eco-Efficient Concrete* Elsevier. pp. 386–436.

Fruhwirth O., Herzog G. W., Hollerer I. and Rachetti a. (1985) Dissolution and hydration kinetics of MgO. *Surf. Technol.* **24**, 301–317.

Hall D. A., Stevens R. and El-Jazairi B. (2001) The effect of retarders on the microstructure

and mechanical properties of magnesia–phosphate cement mortar. *Cem. Concr. Res.* **31**, 455–465. Available at: https://www.sciencedirect.com/science/article/abs/pii/S0008884600005019 [Accessed March 27, 2020].

Hanus L. H., Hartzler R. U. and Wagner N. J. (2001) Electrolyte-induced aggregation of acrylic latex. 1. Dilute particle concentrations. *Langmuir* **17**, 3136–3147.

Jin Y. and Stephan D. (2019) Colloidal interaction between vinylacetate ethylene latex stabilized by polyvinyl alcohol and portland cement. *SN Appl. Sci.* **1**, 129.

Knapen E. and Van Gemert D. (2015) Polymer film formation in cement mortars modified with water-soluble polymers. *Cem. Concr. Compos.* **58**, 23–28.

Kofina A. N., Demadis K. D. and Koutsoukos P. G. (2007) The Effect of Citrate and Phosphocitrate On Struvite Spontaneous Precipitation. *Cryst. Growth Des.* **7**, 2705–2712.

Lavelle J. A. (1988) Acrylic latex-modified Portland cement. *ACI Mater. J.* **85**, 41–48.

Lu Z., Kong X., Zhang C. and Cai Y. (2018) Effect of highly carboxylated colloidal polymers on cement hydration and interactions with calcium ions. *Cem. Concr. Res.* **113**, 140–153.

Merlin F., Guitouni H., Mouhoubi H., Mariot S., Vallée F. and Van Damme H. (2005) Adsorption and heterocoagulation of nonionic surfactants and latex particles on cement hydrates. *J. Colloid Interface Sci.* **281**, 1–10.

Mills D. K. (2018) The Role of Polymer Additives in Enhancing the Response of Calcium Phosphate Cement. In *Orthopedic Biomaterials* Springer International Publishing, Cham. pp. 345–379.

Mohammed S., Daniels E. S., Sperling L. H., Klein A. and El-Aasser M. S. (1997) Isocyanate-functionalized latexes: Film formation and tensile properties. *J. Appl. Polym. Sci.* **66**, 1869–1884.

Ohama Y. (1987) Principle of latex modification and some typical properties of latex-modified

mortars and concretes adhesion; binders (materials); bond (paste to aggregate); carbonation; chlorides; curing; diffusion. *Mater. J.* **84**, 511–518.

Ostrowski N., Roy A. and Kumta P. N. (2016) Magnesium Phosphate Cement Systems for Hard Tissue Applications: A Review. *ACS Biomater. Sci. Eng.* **2**, 1067–1083.

Plank J. and Gretz M. (2008) Study on the interaction between anionic and cationic latex particles and Portland cement. *Colloids Surfaces A Physicochem. Eng. Asp.* **330**, 227–233.

Polat S. and Sayan P. (2020) Preparation, characterization and kinetic evaluation of struvite in various carboxylic acids. *J. Cryst. Growth* **531**, 125339.

Prywer J., Mielniczek-Brzóska E. and Olszynski M. (2015) Struvite crystal growth inhibition by trisodium citrate and the formation of chemical complexes in growth solution. *J. Cryst. Growth* **418**, 92–101.

Rosen M. J. and Kunjappu J. T. (2012) *Surfactants and Interfacial Phenomena*., John Wiley & Sons, Inc., Hoboken, NJ, USA.

Rossignolo J. A. and Agnesini M. V. C. (2002) Mechanical properties of polymer-modified lightweight aggregate concrete. *Cem. Concr. Res.* **32**, 329–334.

Schulthess C. P. and Tokunaga S. (1996) Adsorption Isotherms of Poly(vinyl alcohol) on Silicon Oxide. *Soil Sci. Soc. Am. J.* **60**, 86–91.

Sotiriadis K., Mácová P., Mazur A. S., Tolstoy P. M. and Viani A. (2018) A solid state NMR and in-situ infrared spectroscopy study on the setting reaction of magnesium sodium phosphate cement. *J. Non. Cryst. Solids* **498**, 49–59.

Soudée E. and Péra J. (2000) Mechanism of setting reaction in magnesia-phosphate cements. *Cem. Concr. Res.* **30**, 315–321.

Sugama T. and Kukacka L. E. (1983) Characteristics of magnesium polyphosphate cements derived from ammonium polyphosphate solutions. *Cem. Concr. Res.* **13**, 499–506.

Tian Y., Jin X., Jin N., Zhao R., Li Z. and Ma H. (2013) Research on the microstructure

formation of polyacrylate latex modified mortars. *Constr. Build. Mater.* **47**, 1381–1394.

Tukimat N. N. A., Sarbini N. N., Ibrahim I. S., Ma C. K. and Mutusamy K. (2017) Fresh and Hardened State of Polymer Modified Concrete and Mortars - A Review. *MATEC Web Conf.* **103**.

Viani A. and Gualtieri A. F. (2014) Preparation of magnesium phosphate cement by recycling the product of thermal transformation of asbestos containing wastes. *Cem. Concr. Res.* **58**, 56–66.

Viani A., Lanzafame G., Chateigner D., El Mendili Y., Sotiriadis K., Mancini L., Zucali M. and Ouladdiaf B. (2020) Microstructural evolution and texture analysis of magnesium phosphate cement. *J. Am. Ceram. Soc.* **103**, 1414–1424.

Viani A. and Mácová P. (2018) Polyamorphism and frustrated crystallization in the acid–base reaction of magnesium potassium phosphate cements. *CrystEngComm* **20**, 4600–4613.

Viani A., Mali G. and Mácová P. (2017) Investigation of amorphous and crystalline phosphates in magnesium phosphate ceramics with solid-state 1H and 31P NMR spectroscopy. *Ceram. Int.* **43**, 6571–6579.

Viani A., Peréz-Estébanez M., Pollastri S. and Gualtieri A. F. (2016a) In situ synchrotron powder diffraction study of the setting reaction kinetics of magnesium-potassium phosphate cements. *Cem. Concr. Res.* **79**.

Viani A., Radulescu A. and Peréz-Estébanez M. (2015) Characterisation and development of fine porosity in magnesium potassium phosphate ceramics. *Mater. Lett.* **161**, 628–630.

Viani A., Sotiriadis K., Šašek P. and Appavou M.-S. (2016b) Evolution of microstructure and performance in magnesium potassium phosphate ceramics: Role of sintering temperature of MgO powder. *Ceram. Int.* **42**.

Wang P. H. and Pan C.-Y. (2002) Preparation of styrene/acrylic acid copolymer microspheres: polymerization mechanism and carboxyl group distribution. *Colloid Polym. Sci.* **280**, 152–

159.

Wang P. M., Zhang G. F. and Zhang Y. M. (2005) Influence of polymer powders on mechanical properties of cement mortar. *New Build Mater.* **1**, 32–36.

Wang R., Wang P.-M. and Li X.-G. (2005) Physical and mechanical properties of styrene–butadiene rubber emulsion modified cement mortars. *Cem. Concr. Res.* **35**, 900–906.

Wei L., Hong T., Li X., Li M., Zhang Q. and Chen T. (2019) New insights into the adsorption behavior and mechanism of alginic acid onto struvite crystals. *Chem. Eng. J.* **358**, 1074–1082.

William Kajjumba G., Emik S., Öngen A., Kurtulus Özcan H. and Aydın S. (2019) Modelling of Adsorption Kinetic Processes—Errors, Theory and Application. In *Advanced Sorption Process Applications* IntechOpen.

Wilson A. D. and Nicholson J. W. (1993) *Acid-base cements. Their biomedical and industrial applications*., Cambridge University Press, Cambridge.

Yeliseyeva V. I., Petrova S. A. and Zuikov A. V (1973) Peculiar features of emulsion copolymerization with functionally substituted water-soluble comonomers. In *Journal of Polymer Science: Polymer Symposia* Wiley Online Library. pp. 63–72.

Zárybnická L., Machotová J., Mácová P., Machová D. and Viani A. (2021a) Design of polymeric binders to improve the properties of magnesium phosphate cement. *Constr. Build. Mater.* **290**, 123202.

Zárybnická L., Mácová P. and Viani A. (2021b) Properties enhancement of magnesium phosphate cement by cross-linked polyvinyl alcohol. *Ceram. Int.*

Zhang G. F., Wang P. M. and Wu J. G. (2004) Influence of polymer powder on the bulk density and capillary water adsorption of cement mortar. *New Build Mater.*, 29–31.

Zhang H., Zhou Z., Yang B. and Gao M. (2003) The Influence of Carboxyl Groups on the Photoluminescence of Mercaptocarboxylic Acid-Stabilized CdTe Nanoparticles. *J. Phys.*

Chem. B **107**, 8–13.

Zhang S., Shi H. S., Huang S. W. and Zhang P. (2013) Dehydration characteristics of struvite-K pertaining to magnesium potassium phosphate cement system in non-isothermal condition. *J. Therm. Anal. Calorim.* **111**, 35–40.